Annals of Physics 417 (2020) 168141

Contents lists available at ScienceDirect

Annals of Physics

journal homepage: www.elsevier.com/locate/aop

Pair correlation in nano systems☆

Vladimir Z. Kresin [a,*], Yurii N.Ovchinnikov [b,c]

[a] Lawrence Berkeley Laboratory, University of California, Berkeley CA 94720, USA
[b] Max-Planck Institute for Physics of Complex Systems, Dresden, 01187, Germany
[c] L. Landau Institute of Theoretical Physics, 117334, Moscow, Russia

ARTICLE INFO

Article history:
Received 4 November 2019
Received in revised form 29 February 2020
Accepted 6 March 2020
Available online 18 March 2020

ABSTRACT

Metallic nanoclusters and aromatic molecules are nano systems which display pair correlation similar to that in usual superconductors. Metallic clusters contain delocalized electrons whose states form energy shells similar to those in atoms or nuclei. Under special but perfectly realistic conditions, superconducting pairing in metallic nanoclusters is very strong. For realistic sets of parameters one can expect a high value of T_c (≳150 K); in principle, it is possible to raise T_c up to room temperature. Electrons in aromatic molecules form a two-dimensional finite Fermi system and also can display phenomena caused by pair correlation.

1. Introduction

We are delighted to contribute this paper to the Special Issue celebrating G. M. Eliashberg's 90th birthday. We are especially pleased by the fact that the famous Eliashberg equation [1] is the key tool which enabled us to carry out the studies described below.

This paper is concerned with the superconducting state in nano systems. It is a mini-review of previous work and additionally contains some new results. We begin by describing the properties of small metallic nanoclusters, which contain ∼hundreds of delocalized electrons. The study of nanoclusters has attracted a lot of attention after the discovery of shell structure in their electronic spectra [2]. Because of this shell structure certain clusters display very high critical temperatures. Potentially, their T_c can reach the room temperature. In the second part we focus on two dimensional nano systems, more specifically on the so-called aromatic molecules.

☆ This article is part of the Special Issue: Eliashberg theory at 60.

* Corresponding author.
E-mail address: vzkresin@lbl.gov (Y. N.Ovchinnikov).

https://doi.org/10.1016/j.aop.2020.168141
0003-4916/

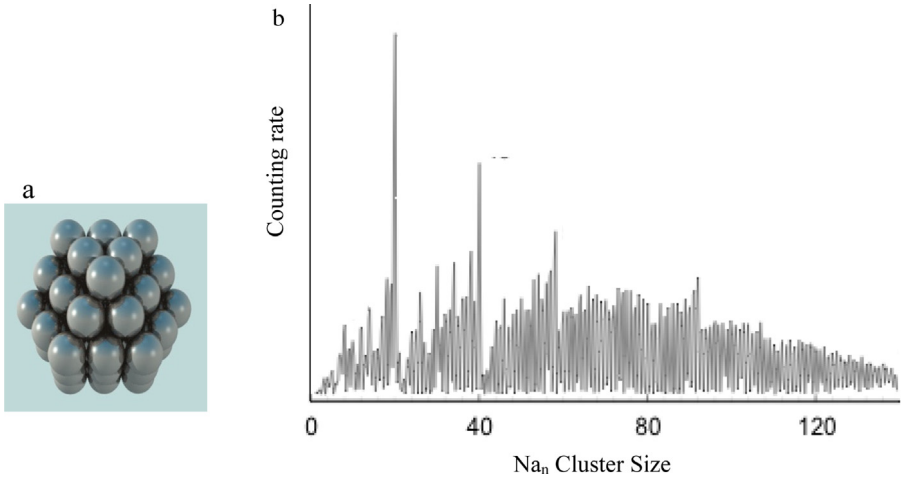

Fig. 1. (a) Cluster; (b) abundance in mass spectra. Vertical axis: number of electrons per cluster (counting; the peaks in stability correspond to "magic" clusters).

2. Metallic nanoclusters

Energy Shells. Clusters are aggregates of atoms with a composition A_k, where k is the number of atoms A (e.g., Na_k, Ga_k, etc.), see Fig. 1a. Metal clusters, like any metallic system, contain delocalized electrons; this subsystem derives from the valence electrons of the atoms. The number of valence electrons, N, is the main parameter, with $N = \nu k$ where ν is the number of valence electrons per atom. For example, for Al_{45} clusters $N = 135$ since each Al atom contains three valence electrons. With the use of mass spectrometry one can focus on clusters of specific masses. It is important to note that because of finite size, the electronic energy spectrum of an isolated cluster is discrete. A milestone discovery made in 1984 in Berkeley [2] demonstrated that the electronic spectra in many metal clusters form energy shells similar to those in atoms or atomic nuclei. For this reason clusters are sometimes called "artificial atoms". The existence of energy shells means that the levels can be classified by their angular momenta L (i.e., s, p, d, f, … shells) with the well-known degeneracy of $g = 2(2L+1)$. Shell structure is the key feature of nanoclusters (see, e.g., the review [3]), Fig. 1b.

So-called "magic number" clusters are most stable. Similarly to inert atoms, they have fully occupied electronic energy shells. Examples of magic numbers include $N_m = 2, 8, 20, 40, 132, \ldots$ The highest occupied shell (HOS) and the lowest unoccupied shell (LUS) are analogous to the HOMO and LUMO orbitals in molecular spectroscopy. Importantly, "magic" clusters are, to a good accuracy, spherically symmetric. Their electronic states can be classified by the angular momentum L and radial n quantum numbers.

If the energy shell is incompletely filled, the cluster undergoes a Jahn–Teller distortion and its shape is non-spherical. This splits energy levels with specific values of L, so that the electronic states of deformed clusters are classified not by L, but by the projection of the angular momentum m. The scale of splitting depends on the individual cluster. Since the change in shape affects the electronic energy spectrum, one finds a unique correlation between the number of electrons and the energy spectrum. This feature makes metallic clusters quite remarkable.

2.1. Superconducting state and critical temperature. High T_c

Cooper pairs in bulk superconductors are formed by electrons with opposite momenta and spins. For nanoclusters momentum is not a good quantum number, and pairs are formed by electrons with opposite projections of the angular momentum $(m, -m)$.

In many aspects metal nanoclusters are analogous to atomic nuclei. Both cases involve finite Fermi systems and the presence of shell structure. The pairing picture is also similar (see, e.g., [4,5]), and the pairing states are labeled by similar quantum numbers $(m, -m)$. However, for clusters one can develop a fully microscopic approach. This is the case because the forces are known precisely (Coulomb interaction) and in addition one can employ the adiabatic approximation and introduce the effects of non-adiabaticity, that is to say, the electron–vibrational interaction. Moreover, one can increase the size of the cluster continuously and trace its evolution all the way to a bulk solid. As a result, one is able to make use of some bulk parameters (of course, with proper scaling). This is important for the analysis of the superconducting state in nanoclusters.

Let us begin by discussing pairing in isolated clusters [6]. The equation for the pairing order parameter $\Delta(\omega_n)$ has the following form:

$$\Delta(\omega_n) Z = \eta \frac{T}{2V} \sum_{\omega_{n'}} \sum_{s} D(\omega_n - \omega_{n'}) F_s^+(\omega_{n'}) \tag{1}$$

Here $\omega_n = (2n+1)\pi T$; $n = 0, \pm 1, \pm 2, \ldots$;

$$D\left(\omega_n - \omega_{n'}, \tilde{\Omega}\right) = \tilde{\Omega}^2 \left[(\omega_n - \omega_{n'})^2 + \tilde{\Omega}^2\right]^{-1};$$
$$F_s^+(\omega_{n'}) = \Delta(\omega_{n'}) \left[\omega_{n'}^2 + \xi_s^2 + \Delta^2(\omega_{n'})\right]^{-1} \tag{1'}$$

are the vibrational propagator and the Gor'kov pairing function [7], respectively, $\xi_s = E_s - \mu$ is the energy of the sth electronic state referred to the chemical potential μ, $\tilde{\Omega}$ is the characteristic vibrational frequency, V is the cluster volume, $\eta = \langle I \rangle^2 / M\tilde{\Omega}^2$ is the so-called Hopfield parameter (see, e.g., [8]), and Z is the renormalization function. We employ the thermodynamic Green's function method (see, e.g., [9]).

Electron-vibrational interaction is considered as the major mechanism of pairing. The general equation (1) explicitly contains the vibrational propagator. This equation is used because we wish to go beyond the restriction $T_c \ll \tilde{\Omega}$ (weak coupling approximation).

Eq. (1) is similar to the Eliashberg equation [1]. Since it is applied to a nanoscale system, it involves a summation over the discrete energy levels E_S. Another important aspect in dealing with a finite Fermi system is that the number of electrons N is fixed. Consequently the position of the chemical potential differs from the Fermi level E_F and is determined by the values of N and T. Specifically, one can write

$$N = \sum_{\omega_n; s} \sum_{s} G_s(\omega_n) e^{i\omega_n \tau}_{|\tau \to 0} = \sum_{s} (u_s^2 \varphi_s^- + v_s^2 \varphi_s^+) \tag{2}$$

Here $G_s(\omega_n)$ is the thermodynamic Green's function,

$$u_s^2, v_s^2 = 0.5\left(1 \mp \frac{\xi_s}{\varepsilon_s}\right); \varphi_s^{\mp} = \left[1 + \exp\left(\mp \frac{\varepsilon_s}{T}\right)\right]^{-1};$$
$$\varepsilon_s = \left(\xi_s^2 + \varepsilon_{0;s}^2\right)^{\frac{1}{2}} \tag{2'}$$

$\varepsilon_{0;s}$ is the pairing gap parameter for the sth level; and $\varepsilon_{0;s}$ is the root of the equation $\varepsilon_{0;s} = \Delta(-i\varepsilon_s)$. Since $\xi_s = E_s - \mu$, Eq. (2) determines the position of the chemical potential for a given electron number N, as well as the dependence $\mu(T)$. These dependences are important for the study of pairing in clusters.

Eqs. (1) and (2) are the main equations of the theory, allowing to evaluate the critical temperature and the energy spectrum. At $T = T_C \Delta$ should be set to zero in the denominator of the expression (1′). One can show that $\eta = \lambda_b / \nu_b$, where λ_b and ν_b are the bulk values of the coupling constant and the density of states [6]. It is essential that these equations involve experimentally measured parameters: N (the number of delocalized electrons), E_F, $\tilde{\Omega}$, the degeneracy g_i, λ_b, and the energy spectrum (ξ_i). This makes it possible to calculate the critical temperatures for various clusters.

This calculation can be performed by means of a matrix method [10,11]. It reveals that a high value of T_c can be obtained for perfectly realistic parameter values. For example, if we consider a

"magic" cluster with the following parameters: $\Delta E = E_H - E_L = 65$ meV, $\tilde{\Omega} = 25$ meV, $m^* = m_e$, $k_F = 1.5 \times 10^8$ cm^{-1}, $\lambda_b = 0.4$, the radius $R = 7.5$ Å, and $g_H + g_L = 48$ (e.g., $L_H = 7$, $L_L = 4$), we arrive at $T_C \cong 10^2$ K (!). Note that the large degeneracy of LUS and HOS plays a key role.

The value of T_c is very sensitive to the cluster parameters. The most favorable case corresponds to a cluster with

(1) high orbital momenta L for the highest occupied and lowest unoccupied shells, and hence with large degeneracies g_{HUS} and g_{LOS} (qualitatively, this corresponds to a large effective density of states);

and

(2) relatively small energy spacing between these shells.

T_c can be increased by changing the parameters (ΔE, $\tilde{\Omega}$, etc.) in the desired direction. For example, for $\Delta E \cong 0.2$ eV, $\lambda_b = 0.5$, $m^* \cong 0.5 m_e$, $R \cong 5.5$ A, $\widetilde{\Omega} = 50$ meV, $g_H + g_L = 60$, we obtain $T_c \cong 240$ K (!). In principle, T_c can be increased to room temperatures.

Based on Eqs. (1), (2) one can calculate T_c for specific clusters. The results vary noticeably depending on their parameters. For example, consider Al_{56}. It contains $N = 168$ electrons. This is a "magic" cluster with the highest occupied shell (HOS) corresponding to $L = 7$. Indeed, according to [12], for $N = 168$ one observes a sharp drop in the ionization potential. The next "magic" cluster contain $N = 198$ electrons and corresponds to hybridization of three shells with $L = 4$, $n = 2$; $L = 2$, $n = 2$; and $L = 0$, $n = 4$; as a result $g_H + g_L = 60$. The spacing between HOS and LUS is $\Delta E \approx 0.1$ eV. Using the parameters for Al_{56} clusters ($R \approx 6.5$ Å, $\widetilde{\Omega} = 350K$, $\lambda_b = 0.4$, $m^* = 1.4$ m_e, $k_F = 1.7 \times 10^8$ cm^{-1}), we obtain for these clusters $T_c \cong 90$ K (!). Similarly, one can expect the critical temperature ($T_c \simeq 100 - -120$ K) for the "magic" cluster Al_{66} as well to greatly exceed that for bulk samples ($T_{c;Bulk} \cong 1.1$ K).

Therefore, the value of T_c is high. Qualitatively, this can be understood as follows. Consider the case when the highest occupied shell is highly degenerate, i.e., $2(2L+1)$ is large. This can be viewed as a sharp peak in the density of states at the Fermi level. The situation is similar to that studied in [13] for bulk materials: the presence of a peak in the density of states (van Hove singularity) results in a noticeable increase in T_c. It is essential that the density of states in the clusters of interest has a strong peak at the Fermi level.

2.2. Finite systems and coherence length

The study of superconducting nanoparticles has attracted a lot of interest. Experiments performed by Tinkham et al. [14] (see the review [15]) with the use of tunneling spectrometry have revealed many interesting features. However, the nanoparticles in that work were large (50–100 Å diameter, containing $\sim 10^4$–10^5 electrons). In contrast, here we are concerned with much smaller particles: nanoclusters containing $\sim 10^2$ electrons. This is the scale at which shell structure, which is the key ingredient of our analysis, has been observed. It is important to emphasize that our analysis is based on Eq. (1) which allows us to go beyond the weak coupling approximation and to obtain solutions corresponding to high values of T_c. For this reason the Richardson model [16] (see the review [17]) based on the Bardeen Hamiltonian with a four-fermion interaction is not applicable here: such Hamiltonian corresponds to the weak coupling limit. Note also that the treatment [18] was based on the assumption that the energy levels are approximately equidistant. With shell structure this assumption is invalid, since here we deal with highly degenerate levels or with groups of very close levels. Because of the high value of T_c, the coherence length is short (this is similar to the situation with high T_c cuprates) and comparable with the cluster size. As a result, broadening due to fluctuations is relatively small [6], on the order of $(\delta T_C/T_C) \approx 5\%$. The study of the parity parameter [19] is concerned with large nanoparticles investigated in [14] and the impact of fluctuations on it. The presence of the shell structure in small nanoclusters leads to a different picture.

Note also that although we talk about a phase transition into the superconducting state, rigorously speaking such a transition can be defined only for infinite systems, since it is for such systems that a singularity in the thermodynamic potential or ins derivative can be defined. Nevertheless, one can consider regions with pair correlation, and a transition to the macroscopic scale allows one to define the critical temperature exactly.

Fig. 2. Cluster-based tunneling network.

2.3. Nano-based tunneling networks

Josephson tunneling between nanoclusters can set up a macroscopic supercurrent [20], Fig. 2. Such Josephson tunneling between clusters needs to be analyzed with considerable care due to the fact that clusters possess discrete energy spectra as opposed to usual bulk superconductors. It cannot be treated with the use of the tunneling Hamiltonian. It is important to take into account the shell degeneracies. As demonstrated in [20], tunneling charge transfer indeed is realistic and in fact provides a drastic increase in the current amplitude relative to the usual bulk case. Note also that although the phase of an isolated cluster does not have a specific value, because of the fixed number of electrons, a phase difference can be defined [21].

A new type of 3D crystals ("cluster metals") can be created by using metal nanoclusters as building blocks. Such solids would be analogous to molecular crystals. The presence of pair correlation in an isolated cluster will lead to Josephson charge transfer between neighboring clusters; as a result, such a cluster-based 3D crystal will display macroscopic superconductivity. The concept of such a superconducting crystal was introduced in [22].

2.4. How to observe the phenomenon?

Pairing results in a strong temperature dependence of the excitation spectrum. Below T_c and especially at low temperatures close to $T = 0$ K, the excitation energy becomes strongly modified by pairing so as to noticeably exceed its value for $T > T_c$. In addition, pairing produces an increase in the electronic density of states near the energy gap. A change in the excitation energy and a redistribution of levels should be experimentally observable and would provide strong manifestation of pair correlation. Such an effect has been observed experimentally in [23,24] for Al_{66}. This is not an accident, because Al_{66} is a "magic" cluster with a large angular momentum (hence, degeneracy) of its HOS and LUS.

The transition into a pairing state is a phase transition and should be accompanied by a jump in heat capacity. An interesting calorimetric study, based on an induced dissociation method, was carried out in [25], finding a peak was observed for Al_{45}^- ions. It is again important that this additional peak is not universal and can be observed only for certain selected clusters. The peak was observed at $T \approx 200$ K(!); according to the authors [25] the result is highly reproducible. This observation is also very informative.

3. 2D nano systems. Aromatic molecules

In this section we describe another example of small scale systems, so-called conjugated hydrocarbons, or, more specifically, aromatic molecules. The molecules are planar but otherwise are similar to metal clusters. They contain so-called π-electrons which are delocalized and moving in the field created by the σ-core; the σ-core is formed by the ionic system and the other electrons. Each carbon atom supplies one such delocalized π-electron. As an example, the coronene molecule $C_{24}H_{12}$ (Fig. 3a) contains 24 π-electrons. As noted, the π-electrons have similarities to conduction electrons in metals; only in this case we are again dealing with a finite Fermi-system.

The benzene molecule (see the Appendix) is the major building block of these structures. Below we focus on the π-electrons states of the coronene molecule and their spectrum.

π-electrons can form Cooper pairs, bringing the molecules into the superconducting state. This concept was introduced in [26,27]. Here we describe the picture and present some new results. Of course, since an isolated aromatic molecule is a small system it is meaningless to talk about its

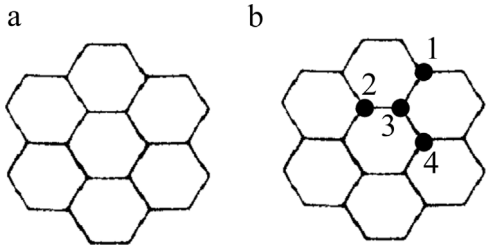

Fig. 3. (a) Coronene molecule (the hydrogen ions are omitted for clarity); (b) location of the selected ions.

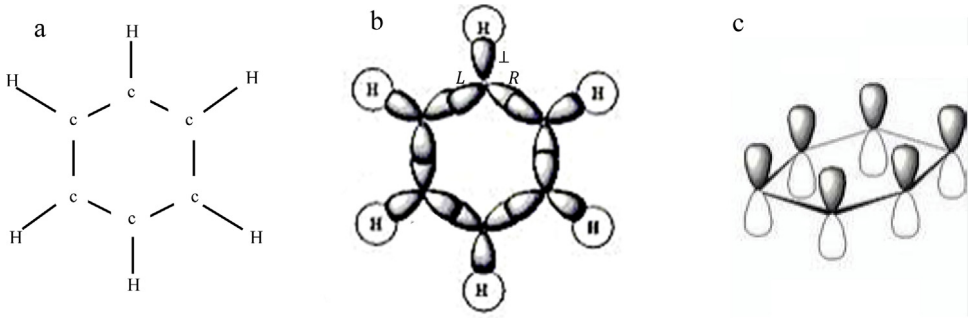

Fig. 4. (a) Benzene molecule; (b) in-plane atomic orbitals; (c) p_z atomic orbitals.

conductivity and zero resistance. But pair correlation similar to that in the usual superconductors does exist and manifests itself in various phenomena.

We begin by evaluating the electronic energy spectrum of the molecule (in the absence of pair correlation). The method takes advantage of the symmetry of the molecule (D_{6h}) and its periodicity with respect to rotation with period $\tilde{\varphi} = \pi/3$. More specifically, let us select the set of four carbon ions marked in Fig. 3b. By consecutive $\pi/3$ rotations of this set relative to the axis we cover the full structure of the molecule. This allows us to seek the total electronic wave function as a sum (cf. Eq. (A.1)):

$$\Psi(\mathbf{r}) = \sum_s e^{im\varphi^s}\{\alpha\Psi^{(1)} + \beta\Psi^{(2)}e^{i\varphi_2} + \gamma\Psi^{(3)}e^{i\varphi_3} + \mu\Psi^{(4)}e^{i\varphi_4}\}_s \tag{3}$$

Here; $s = 1, 2, \ldots,$ $\psi^{(i)}$ corresponds to the ith ion in the set, and $\varphi_2, \varphi_3, \varphi_4$, are the relative phase factors. Substituting expression (3) into the Schrödinger equation, we obtain the secular equation

$$\|S_{ik}\| = 0, i, k = 1, 2, \ldots, 4 \tag{4}$$

Here $S_{11} = \mathrm{E} - 2\mathrm{T_z}\cos m\tilde{\varphi}$, $S_{ii} = \mathrm{E}$, $S_{12} = S_{21}^* = -\mathrm{T_z}\exp(i\varphi_2)$; $S_{2k} = S_{k2}^* = -\mathrm{T_z}\exp[i(\varphi_k - \varphi_2)]$; $S_{34} = S_{43} = -\mathrm{T_z}\exp[im\tilde{\varphi} + \varphi_4 - \varphi_3]$, $S_{13} = S_{31} = S_{14} = S_{41} = 0$; we have set $\varepsilon_0 = 0$.

Eq. (4) can be written in the following form:

$$Z^4 - 2Z^3\cos m\tilde{\varphi} - 4Z^2 - 4Z\cos m\tilde{\varphi} + (1 + 4\cos 2m\tilde{\varphi}) = 0 \tag{4'}$$

where $Z = \mathrm{E}/\mathrm{T_z}$.

The energy spectrum (in units of $\mathrm{T_z}$) is described by Eq. (4). It is interesting that the spectrum is symmetric relative to the chemical potential ($\varepsilon_0 = 0$). The energy distribution of all 24 π-electrons can be also shown. The value of the parameter $\mathrm{T_z}$ can be taken from experimental data on the benzene molecule ($\simeq$350 meV). The excitation energy, referred to chemical potential placed in the middle of the HOMO-LUMO interval, works out to be on order of $\simeq$175 meV. This value is

noticeably lower than the vibration energy of the hydrogen ion (∼200–250 meV). The presence of high frequency hydrogen modes is the key factor that makes π-electrons pairing perfectly realistic. The situation is similar to pairing in the hydrides [28] caused by the interaction of conduction electrons with high frequency hydrogen phonon modes [29–31].

Let us discuss the manifestations of pairing. That is, we summarize experimental observations which lead one to the conclusion that the π-electrons in the coronene molecule indeed form Cooper pairs.

To recap, the energy spectrum plotted in Fig. 4 is evaluated directly from the Schrodinger equation without accounting for any pair correlations. One can see that the quantities $\omega_{0-0'}$ and $\omega_{0'-0''}$, which correspond to excitations of the first and second levels, are of the same order of magnitude. However, the experimental data presents a different picture. For the coronene molecule $\omega_{0-0'} \simeq 22.5 \times 10^3\ \mathrm{cm}^{-1}$, whereas $\omega_{0'-0''} \simeq 5.5 \times 10^3\ \mathrm{cm}^{-1}$ [32] . This very significant difference can be explained if pair correlation is present and gives rise to the corresponding pairing energy gap, which affects the energy spectrum and drastically increases the lowest excited level.

It is interesting that for the ion $C_{24}H_{13}^-$, which contains an odd number of electrons, a large reduction of the $0 - 0'$ separation is observed [33]. This is natural in the above picture, since this ion contains an unpaired electron (the odd–even effect).

As is known, in ordinary metals the paramagnetic χ_P and diamagnetic χ_D terms nearly cancel each other, leaving only the small residual Landau diamagnetism. In superconductors, on the other hand, the presence of the gap parameter suppresses the paramagnetic term and leads to the well-known anomalous diamagnetism (Meissner effect). In molecular systems both χ_P and χ_D must be evaluated, since they are of the same order of magnitude. However, the aromatic molecules of interest display strong diamagnetic response (for example, for coronene $\chi \equiv \chi_D \simeq -2.4 \times 10^{-4}\ \mathrm{cm}^3/\mathrm{mol}$). This implies that the paramagnetic term is small due to the pairing order parameter Δ.

The manifestation of pairing in aromatic molecules is similar to that for nucleons (protons and neutrons) in atomic nuclei which is a well-established concept in nuclear physics (see, e.g., [4,5]). This is not surprising, because in both cases we deal with a finite Fermi system. Both systems (nuclei and aromatic molecules) interact with radiation in an analogous way. As is known, the spectroscopy of usual bulk superconductors is greatly affected by the opening of the energy gap at $T = T_c$. For the systems discussed here, their finite size makes their spectra discrete even in the absence of pair correlation. However, as elucidated above, because of pairing the energy spacing between the ground state and the first excited state (the so-called 0-0′ transition) greatly exceeds that between the first and second excited states (the 0′-0″ transition). In addition, the odd–even effect can be observed: the light absorption threshold is much lower for a system with an odd number of electrons because of the presence of one unpaired particle.

Pair correlation of nucleons results in a decrease of nuclear moments of inertia relative to the rigid body configuration. This phenomenon is similar to anomalous diamagnetism, because transition to a rotating coordinate system is equivalent to the appearance of an external magnetic field (see, e.g., [34]).

As pointed out above, the key ingredient enabling the pairing of π-electrons in the molecules of interest is the presence of hydrogen ions with high-frequency vibrational modes. Since pairing is caused by electron coupling to these hydrogen modes, the gap parameter and, consequently, the structure of the electronic spectrum must be sensitive to the H $\rightarrow$ D isotope substitution. The observation of such an isotope effect would reveal the presence of the pairing phenomenon in their π-electron systems and validate our prediction.

Declaration of competing interest

The authors declare that they have no known competing financial interests or personal relationships that could have appeared to influence the work reported in this paper.

Acknowledgments

The authors are grateful to L. Gor'kov, J. Friedel, and V. V. Kresin for many fruitful discussions.

Appendix. Methods: Benzene molecule

The benzene molecule C_6H_6 (Fig. 4a) is a basic hydrocarbon molecule, of key importance among organic systems. Because of its simple structure and symmetry, this molecule plays a role similar to that of hydrogen in atomic physics. In addition to the carbon and hydrogen ions, it contains 30 valence electrons which are not bound to the ions and can move in the field formed by the ionic system and other electrons. It is also well known that these valence electrons are separated into two groups:

(1) π-electrons, which are delocalized and move along the ring and (2) σ-electrons. The ionic system and these σ-electrons form the so-called σ- core which creates the background potential for the delocalized motion of the π-electrons. While this separation into π and σ groups works well in molecular spectroscopy, it must be proven rigorously.

Studies of aromatic molecules with structures analogous to benzene focus mainly on the properties of π-electrons. Based on the symmetry of the molecule, one can evaluate rigorously the full energy spectrum of the entire valence electron population of the molecule. One can show (see below) that it contains several groups (branches) of level. Some of them are fully occupied (σ^- and μ^- branches), whereas the group corresponding to the so-called π-states is only partially occupied. The structure of the spectrum and its treatment are similar to that in solids with their valence and conducting bands.

Below we show how the system of valence electrons in the benzene molecule can be analyzed without any *a priori* separation into groups. As will be seen, the analogy with the energy band picture in solids is of key importance.

Let us start from an isolated C atom. It has four valence electrons with the structure $(1s^2)(2s)(2p_x)(2p_y)(2p_z)$ (see, e.g., [35]). As usual, it is convenient to introduce linear combinations of the atomic wave functions, resulting in four orthogonal wave functions (atomic orbitals), see Fig. 4b.

The full C_6H_6 molecule has D_{6h} symmetry. It is invariant with respect to rotations by $\pi/3$ relative to the Z-axis (the Z-axis passes through the center of the molecule and is normal to the molecular plane). In total, we are dealing with 30 valence electrons (24 electrons from the six carbon atoms and 6 electrons from the H atoms). Each of these electrons is delocalized in the field formed by the ionic core made up of six C^{4+} ions, six protons (H^+), and the other electrons.

Now one can employ the tight-binding approximation. As is known, translational symmetry in solids allows the electronic wave function to be written in the Bloch form that depends on the quasi-momentum quantum number. For the benzene molecule with its electronic states periodic with respect to $\pi/3$ rotations, it is reasonable to introduce a "quasi-projection of the angular momentum". This quantity is similar to the quasi-momentum in crystals and reflect the rotational periodicity. Correspondingly, the electronic wave function can be sought in the form:

$$\Psi\left(\overrightarrow{r}\right) = \sum_s e^{im\varphi_s}[\alpha_m\psi_L^s + \beta_m\psi_R^s + \mu_m\psi_{\perp}^s + \eta_m\psi_H^s + \gamma_m\psi_Z^s] \tag{A.1}$$

Here, s corresponds to isolated C ions, and $i \equiv \{L, R, \perp, H, Z\}$ denotes the orbitals (see Fig. 4b, c).

Eq. (A.1) is analogous to the form used in solid state theory for the case of degenerate energy levels (see, e.g., [36] and also [37]). A similar equation has been used in the theory of manganites [38] developed by Gor'kov and one of the authors, where the band structure is described in the tight-binding approximation and reflects the degeneracy of the Mn ions.

Substituting expression (A.1) into the Schrodinger equation $\hat{H}\Psi = E\Psi$, multiplying it by $\Psi_i^{(L)}$ and integrating, we obtain the general secular equation

$$|S_{ik}| = 0. \tag{A.2}$$

Here $S_{11} = S_{22} = E - \varepsilon_o$, ε_o is the energy of the upper occupied electronic term of an isolated carbon atom (we set $\varepsilon_o = 0$), $\widetilde{\varphi} = \pi/3$, $m = 0, \ldots, 3$,

$$T_p \equiv T_{RL}^{1;2} \equiv T_{LR}^{1;6} = \int \psi_R^{(1)}\tilde{V}\psi_L^{(2)}d\boldsymbol{r},$$

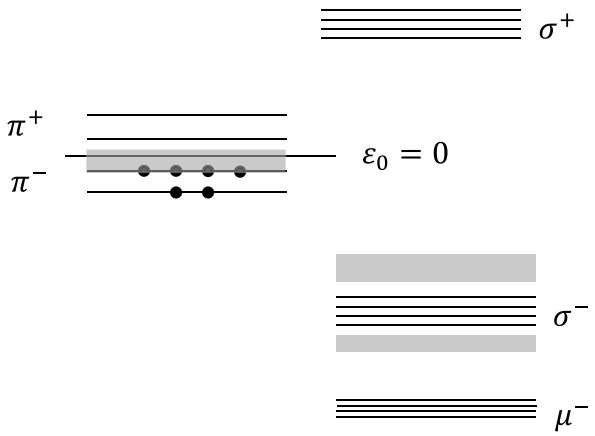

Fig. 5. Energy spectrum of the C_6H_6 molecule. Black dots and gray areas denote the occupied energy levels.

$\tilde{V} = V - \nu(\boldsymbol{r_s})$, $\nu(\boldsymbol{r_s})$ is the potential of an isolated C ion Further, $S_{33} = E - \tilde{\varepsilon}_0$; $\tilde{\varepsilon}_0 = \varepsilon_0 + 2T_\perp \cos m\tilde{\varphi}$; $T_\perp = \int \psi_\perp^{(1)} \tilde{v} \psi_\perp^{(2)} d\vec{r}$; $S_{44} = E - \varepsilon_H$, ε_H is the lowest electronic term of hydrogen, and $S_{55} = E - (\varepsilon_0 + 2T_z \cos m\tilde{\varphi})$, where

$$T_z = \int \psi_z^{(1)} \tilde{V} \psi_z^{(2)} d\vec{r} \tag{A.2′}$$

The matrix elements T_Z, T_P, etc., describe electron tunneling between neighboring ions. This tunneling splits the electronic levels of an isolated C ion. We neglect overlap integrals containing direct products of electronic wavefunctions from neighboring ions.

In the first approximation we neglect small terms such as $T_{p;\perp} = \int \psi_z^{(1)} \tilde{V} \psi_z^{(2)} d\vec{r}$, S_{13},etc.

The secular equations (A.2) has five roots which means that there are five groups (branches) of energy levels (see below). Each of these groups contains 4 levels; of which two are doubly degenerate ($m = 1,-1$ and $2,-2$) and can accommodate 4 electrons each. On the whole, each branch can accommodate 12 electrons.

An essential point is that because the functions $\psi_z^{(1)}$ are antisymmetric with respect to reflection in the plane of the molecule and the other orbitals and the operator $T \equiv \tilde{V}$ are symmetric, all the elements $S_{i4} = S_{4i} = 0$, and one branch can be determined immediately (cf. [39]), it arises from the tunneling between the electronic ψ_z states belonging to neighboring C ions. Therefore one group of levels can be immediately identified:

$$E_1 = 2\mathrm{T_z} cos m\tilde{\varphi} \tag{A.3}$$

As noted above, we assumed $\varepsilon_0 = 0$.

Other branches can be also determined from the secular equation. It is easy to find that:

$$E_{2,3} \approx \pm \mathrm{T_p} \tag{A.4}$$

These groups form σ ($=-\mathrm{T_p}$) and σ^+ ($=\mathrm{T_p}$) energy levels. If we take into account small tunneling terms such as $\mathrm{T_{p;\_|\_}}$, then this energy level will be slightly split.

Finally, the energy levels E_4 and E_5 are described by the following dispersion relations:

$$\mathrm{E_4} \approx \varepsilon_\mathrm{H};\ \mathrm{E_5} \approx 0 \tag{A.5}$$

These levels form groups E_μ^+ and E_μ^-.

As a result, as mentioned above there are five energy level branches. As noted, each branch contains four energy levels and can accommodate 12 electrons whose states differ in the value of the quasi-projection of angular momentum m and spin.

Fig. 5 shows the structure of the electronic energy spectrum for the benzene molecule.

The total number of valence electrons is 30. According to the Pauli principle, these electrons are distributed among the energy levels plotted in Fig. 5. All the lowest levels (the E_{μ}^{-}levels, all the E_{σ}^{-}levels, and two E_{π}^{-} levels) are occupied. The upper two E_{π}^{+} energy levels and all E_{σ}^{+} and E_{μ}^{+} levels are vacant.

The difference between π and σ electrons is not in delocalization vs localization. Indeed, the wave functions of all valence electrons, including the σ states, are delocalized. The point is that the π and σ states correspond to different parts of the energy spectrum. The σ branch is totally occupied, unlike the π branch which is only partially occupied. For the π branch, intra-branch transitions are allowed. The σ branch is similar to the valence (fully occupied) energy bands in solids, whereas the π electron branch is similar to the conduction bands.

References

[1] G. Eliashberg, JETP 12 (1961) 1000.
[2] W. Knight, K. Clemenger, W. de Heer, W. Saunders, M. Chou, M. Cohen, Phys. Rev. Lett. 52 (1984) 2141.
[3] W. de Heer, Rev. Modern Phys. 65 (1993) 611.
[4] P. Ring, P. Schuck, The Nuclear Many-Body Problem, Springer, NY, 1980.
[5] R. Broglia, V. Zelevinsky (Eds.), Fifty Years of Nuclear BCS, World, Singapore, 2013.
[6] V. Kresin, Y. Ovchinnikov, Phys. Rev. B 74 (2006) 024514.
[7] L. Gor'kov, JETP 7 (1958) 505.
[8] G. Grimvall, The Electron-Phonon Interaction in Metals, Amsterdam: North- Holland, 1981.
[9] A. Abrikosov, L. Gor'kov, I. Dzyaloshinski, Methods of Quantum Field Theory in Statistical Physics, Dover, NY, 1975.
[10] C. Owen, D. Scalapino, Physica 55 (1971) 691.
[11] V. Kresin, H. Gutfreund, W. Little, Solid State Commun. 51 (1984) 12.
[12] K. Schriver, J. Persson, E. Honea, R. Whetten, Phys. Rev. Lett. 64 (1990) 2359.
[13] J. Labbe, S. Baristic, J. Friedel, Phys. Rev. Lett. 19 (1967) 1039.
[14] M. Tinkham, J. Hergenrother, J. Lu, Phys. Rev. B 51 (1995) 12649.
[15] D. von Delft, D. Ralth, Phys. Rep. 345 (2001) 61.
[16] R. Richardson, Phys. Lett. 3 (1963) 277.
[17] J. von Delft, F. Braun, arXiv:cond-mat/99/1058v1, 1999.
[18] P. Anderson, J. Phys. Chem. Solids 11 (1959) 59.
[19] K. Matveev, A. Larkin, Phys. Rev. Lett. 78 (1997) 3749.
[20] Y. Ovchinnikov, V. Kresin, Phys. Rev. B 81 (2010) 214505; Phys. Rev. B 85 (2012) 064518.
[21] D. Cobert, U. Schoolwock, von Delft, Eur. Phys. J. B 38 (2004) 501.
[22] J. Friedel, J.Phys. 2 (1992) 959.
[23] A. Halder, A. Liang, V.V. Kresin, Nano Lett. 15 (2015) 1410.
[24] A. Halder, V.V. Kresin, Phys. Rev. B 92 (2015) 214506.
[25] B. Cao, C. Neal, A. Starace, Y. Ovchinnikov, V. Kresin, M. Jarrold, J. Super. Novel Magn. 21 (2008) 163.
[26] V. Kresin, JETP 34 (1972) 527.
[27] V. Kresin, V. Litovchenko, A. Panasenko, J. Chem. Phys. 63 (1975) 3613.
[28] A. Drozdov, M. Eremets, I. Troyan, V. Ksenofontov, S. Shylin, Nature 525 (2015) 73.
[29] Y. Li, J. Hao, H. Liu, Y. Li, Y. Ma, Sci. Rep. 5 (2014) 9948.
[30] D. Duan, Y. Liu, F. Tian, D. Li, X. Huang, Z. Zhao, H. Yu, B. Liu, W. Tian, Ti Cui, Sci. Rep. 4 (2014) 6968.
[31] L. Gor'kov, V. Kresin, Rev. Modern Phys. 90 (2018) 011001.
[32] E. Clar, Aromatishe Kohlenwasserstoffe, Springer-Verlag, Berlin, 1952.
[33] G. Hotjtiak, P. Zandstra, Mol. Phys. 3 (1960) 371.
[34] L. Landau, E. Lifshits, The Classical Theory of Fields, Pergamon, NY, 1994.
[35] K. Higasi, H. Baba, A. Rembaum, Quantum Organic Chemistry, Wiley, NY, 1965.
[36] A. Anselm, Introduction to Semiconductor Theory, Prentice-Hall, NY, 1982.
[37] M. Dewar, The Molecular Orbital Theory of Organic Chemistry, McGraw-Hill, NY, 1969.
[38] L. Gor'kov, V. Kresin, Phys. Rep. 400 (2004) 149.
[39] E. Hückel, Z. Phys. 70 (1931) 204.